

ASAM: Adaptive Sharpness-Aware Minimization for Scale-Invariant Learning of Deep Neural Networks

Jungmin Kwon*

Jeongseop Kim*

Hyunseo Park*

In Kwon Choi*

Abstract

Recently, learning algorithms motivated from sharpness of loss surface as an effective measure of generalization gap have shown state-of-the-art performances. Nevertheless, sharpness defined in a rigid region with a fixed radius, has a drawback in sensitivity to parameter re-scaling which leaves the loss unaffected, leading to weakening of the connection between sharpness and generalization gap. In this paper, we introduce the concept of adaptive sharpness which is scale-invariant and propose the corresponding generalization bound. We suggest a novel learning method, adaptive sharpness-aware minimization (ASAM), utilizing the proposed generalization bound. Experimental results in various benchmark datasets show that ASAM contributes to significant improvement of model generalization performance.

1 Introduction

Generalization of deep neural networks has recently been studied with great importance to address the shortfalls of pure optimization, yielding models with no guarantee on generalization ability. To understand the generalization phenomenon of neural networks, many studies have attempted to clarify the relationship between the geometry of the loss surface and the generalization performance (Hochreiter et al., 1995; McAllester, 1999; Keskar et al., 2017; Neyshabur et al., 2017; Jiang et al., 2019). Among many proposed measures used to derive generalization bounds, loss surface sharpness and minimization of the derived generalization bound, proved to be effective in attaining state-of-the-art performances in various tasks (Hochreiter & Schmidhuber, 1997; Mobahi, 2016; Chaudhari et al., 2019; Sun et al., 2020; Yue et al., 2020).

*Samsung Research, Seoul, Republic of Korea, Correspondence to: Jeongseop Kim <jisean.kim@samsung.com>.

Especially, sharpness-based minimization (Foret et al., 2020) as a learning algorithm based on PAC-Bayesian generalization bound, achieves a state-of-the-art generalization performance for various image classification tasks benefiting from minimizing sharpness of loss landscape, which is correlated with generalization gap. Also, they suggest a new sharpness calculation strategy, which is computationally efficient, since it requires only a single gradient ascent step in contrast to other complex generalization measures such as sample-based or Hessian-based approach.

However, even the sharpness-based learning methods and some of the sharpness measure suffer from sensitivity to model parameter re-scaling. Dinh et al. (2017) points out that parameter re-scaling which does not change loss functions can cause a difference in sharpness values so this property may weaken correlation between sharpness and generalization gap. We call this phenomenon scale-dependency problem.

To remedy the scale dependency problem of sharpness, many studies have been conducted recently (Liang et al., 2019; Yi et al., 2019; Karakida et al., 2019; Tsuzuku et al., 2020). However, those previous works are limited to proposing only scale-invariant generalization measures and do not provide sufficient investigation on combining learning algorithm with the scale-invariant measures.

To this end, we introduce the concept of normalization operator which is not affected by any scaling operator that does not change the loss function. The operator varies depending on the way of normalizing, e.g., element-wise and filter-wise. We then define *adaptive sharpness* of the loss function, sharpness whose maximization region is determined by the normalization operator. We prove that adaptive sharpness remains the same under parameter re-scaling, i.e., *scale-invariant*. Due to the scale-invariant property, adaptive sharpness shows stronger correlation with generalization gap than sharpness does.

Motivated by the connection between generalization metrics and loss minimization, we propose a novel learning method, adaptive sharpness-aware minimization (ASAM), which adaptively adjusts maximization regions for calculation of generalization bound thus acting uniformly under parameter re-scaling. ASAM minimizes the generalization bound using adaptive sharpness to generalize on unseen data, avoiding the scale dependency issue SAM suffers from.

The main contributions of this paper are summarized as follows:

- We introduce adaptive sharpness of loss surface which is invariant to parameter re-scaling. Adaptive sharpness shows stronger correlation with generalization than sharpness does, which means that adaptive sharpness is more effective measure of generalization gap.
- We propose a new learning algorithm using adaptive sharpness which helps alleviate the side-effect in training procedure caused by scale dependency by adjusting their maximization region with respect to weight scale.
- We empirically show its consistent improvement of generalization performance on image classification tasks using various neural network architec-

tures.

The rest of this paper is organized as follows. Section 2 briefly describes previous sharpness-based learning algorithm, and its scale dependent property is explained in Section 3. In Section 4, we introduce adaptive sharpness which is a scale-invariant measure of generalization gap, and in Section 5, ASAM algorithm is introduced in detail using the definition of adaptive sharpness. In Section 6, we evaluate the generalization performance of ASAM for various models and datasets. We provide the conclusion and future work in Section 7.

2 Preliminary

Let us consider a model $f : X \rightarrow Y$ parametrized by a weight vector \mathbf{w} and a loss function $l : Y \times Y \rightarrow \mathbb{R}_+$. Given a sample $S = \{(\mathbf{x}_1, \mathbf{y}_1), \dots, (\mathbf{x}_n, \mathbf{y}_n)\}$ drawn from data distribution D with i.i.d condition, the training loss can be defined as $L_S(\mathbf{w}) = \sum_{i=1}^n l(\mathbf{y}_i, f(\mathbf{x}_i; \mathbf{w}))/n$. Then, the generalization gap between the expected loss $L_D(\mathbf{w}) = \mathbb{E}_{(\mathbf{x}, \mathbf{y}) \sim D}[l(\mathbf{y}, f(\mathbf{x}; \mathbf{w}))]$ and the training loss $L_S(\mathbf{w})$ represents the ability of the model to generalize on unseen data.

Sharpness-aware minimization (SAM) (Foret et al., 2020) aims to minimize the following PAC-Bayesian generalization error upper bound

$$L_D(\mathbf{w}) \leq \max_{\|\boldsymbol{\epsilon}\|_p \leq \rho} L_S(\mathbf{w} + \boldsymbol{\epsilon}) + h\left(\frac{\|\mathbf{w}\|_2^2}{\rho^2}\right), \quad (1)$$

where the domain of max operator, called maximization region, is an ℓ^p ball with radius ρ for $p \geq 1$. Here, sharpness of the loss function L is defined as

$$\max_{\|\boldsymbol{\epsilon}\|_2 \leq \rho} L_S(\mathbf{w} + \boldsymbol{\epsilon}) - L_S(\mathbf{w}). \quad (2)$$

Since $h(\|\mathbf{w}\|_2^2/\rho^2)$ of the inequality in Equation 1 is a monotonically increasing function with respect to $\|\mathbf{w}\|_2^2$, it can be substituted by ℓ^2 weight decaying regularizer, so the sharpness-aware minimization problem can be defined as the following minimax optimization

$$\min_{\mathbf{w}} \max_{\|\boldsymbol{\epsilon}\|_p \leq \rho} L_S(\mathbf{w} + \boldsymbol{\epsilon}) + \frac{\lambda}{2} \|\mathbf{w}\|_2^2,$$

where λ is a weight decaying factor.

SAM solves the minimax problem by iteratively applying the following two-step procedure for $t = 0, 1, 2, \dots$ as

$$\begin{cases} \boldsymbol{\epsilon}_t = \rho \frac{\nabla L_S(\mathbf{w}_t)}{\|\nabla L_S(\mathbf{w}_t)\|_2} \\ \mathbf{w}_{t+1} = \mathbf{w}_t - \alpha_t (\nabla L_S(\mathbf{w}_t + \boldsymbol{\epsilon}_t) + \lambda \mathbf{w}_t), \end{cases} \quad (3)$$

where α_t is an appropriately scheduled learning rate. This procedure can be obtained by a first order approximation of L_S and dual norm formulation as

$$\begin{aligned}\epsilon_t &= \arg \max_{\|\epsilon\|_p \leq \rho} L_S(\mathbf{w}_t + \epsilon) \\ &\approx \arg \max_{\|\epsilon\|_p \leq \rho} \epsilon^\top \nabla L_S(\mathbf{w}_t) \\ &= \rho \operatorname{sign}(\nabla L_S(\mathbf{w}_t)) \frac{|\nabla L_S(\mathbf{w}_t)|^{q-1}}{\|\nabla L_S(\mathbf{w}_t)\|_q^{q-1}},\end{aligned}$$

and

$$\begin{aligned}\mathbf{w}_{t+1} &= \arg \min_{\mathbf{w}} L_S(\mathbf{w} + \epsilon_t) + \frac{\lambda}{2} \|\mathbf{w}\|_2^2 \\ &\approx \arg \min_{\mathbf{w}} (\mathbf{w} - \mathbf{w}_t)^\top \nabla L_S(\mathbf{w}_t + \epsilon_t) + \frac{\lambda}{2} \|\mathbf{w}\|_2^2 \\ &\approx \mathbf{w}_t - \alpha_t (\nabla L_S(\mathbf{w}_t + \epsilon_t) + \lambda \mathbf{w}_t)\end{aligned}$$

where $1/p + 1/q = 1$ and $|\cdot|$ denotes element-wise absolute value function, and sign also denotes element-wise signum function. It is experimentally confirmed that the above two-step procedure produces the best performance when $p = 2$, which results in Equation 3.

As can be seen from Equation 3, SAM estimates the point $\mathbf{w}_t + \epsilon_t$ at which the loss is approximately maximized around \mathbf{w}_t in a rigid region with a fixed radius by performing gradient ascent, and performs gradient descent at \mathbf{w}_t using the gradient at the maximum point $\mathbf{w}_t + \epsilon_t$.

3 Scale Dependency of Sharpness in Rectifier Neural Networks

In this section, we briefly describe the scale dependency problem of sharpness defined in Equation 2. In Foret et al. (2020), it is experimentally confirmed that sharpness defined in Equation 2 is strongly correlated with the generalization gap. Also they show that SAM helps to find minima which show lower sharpness than other learning strategies and contributes to effectively lowering generalization error.

However, Dinh et al. (2017) show that sharpness which is defined in the rigid spherical region with a fixed radius can have a weak correlation with the generalization gap due to non-identifiability of rectifier neural networks, whose parameters can be freely re-scaled without affecting its output. The scale dependency can be explained as follows.

Let us assume we have a two-layered neural network $f(\mathbf{x}; \mathbf{w})$ connected with ReLU-like activation such as

$$f(\mathbf{x}; \mathbf{w}) = W^{(2)} \operatorname{ReLU}(W^{(1)} \mathbf{x}),$$

where

$$\mathbf{w} = \text{concat}(\text{flatten}(W^{(1)}), \text{flatten}(W^{(2)})).$$

Let us assume

$$\mathbf{w}' = \text{concat}(\text{flatten}(W_a^{(1)}), \text{flatten}(W_a^{(2)})),$$

where

$$W_a^{(1)}[i, :] = aW^{(1)}[i, :]$$

and

$$W_a^{(2)}[:, i] = \frac{W^{(2)}[:, i]}{a},$$

for some i , and the other entries of $W_a^{(1)}$ and $W_a^{(2)}$ are the same as those of $W^{(1)}$ and $W^{(2)}$, respectively. We call this transformation from \mathbf{w} to \mathbf{w}' a -transformation throughout this section. Since ReLU is a scale preserving activation function, we have

$$f(\mathbf{x}; \mathbf{w}) = f(\mathbf{x}; \mathbf{w}').$$

Thus, generalization gaps of $f(\mathbf{x}; \mathbf{w})$ and $f(\mathbf{x}; \mathbf{w}')$ are identical, however, sharpness in a rigid region does not maintain the same value when a -transformation is applied. It is because the maximum loss value in the spherical region around \mathbf{w}' can be changed as shown in Figure 1(a). The interval of the loss contours around \mathbf{w}' becomes narrower but the size of the region remains the same, i.e.,

$$\max_{\|\boldsymbol{\epsilon}\|_2 \leq \rho} L_S(\mathbf{w} + \boldsymbol{\epsilon}) \neq \max_{\|\boldsymbol{\epsilon}\|_2 \leq \rho} L_S(\mathbf{w}' + \boldsymbol{\epsilon}).$$

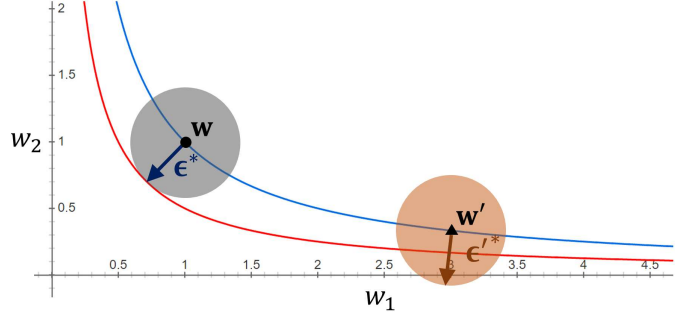
Since both identical neural networks can have arbitrarily different values of sharpness, small sharpness defined in Equation 2 does not necessarily mean a low generalization error, thus leading to weak correlation between generalization error and sharpness.

4 Adaptive Sharpness: Scale-Invariant Measure of Generalization Gap

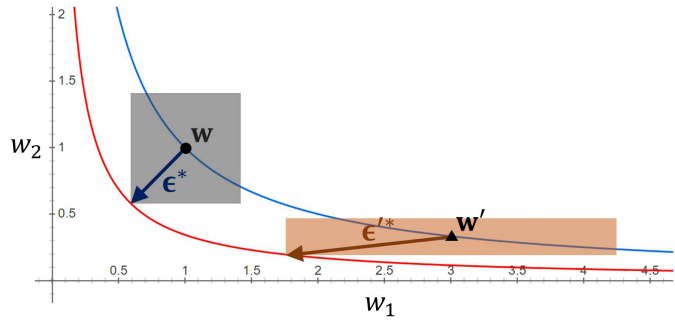
To solve the scale dependency of sharpness defined in Equation 2, we introduce the concept of adaptive sharpness. Prior to explaining adaptive sharpness, we first define normalization operator.

When A is a scaling operator on the weight space that does not change the loss function as in the example in Section 3, the normalization operator that cancels out the effect of A can be defined as follows.

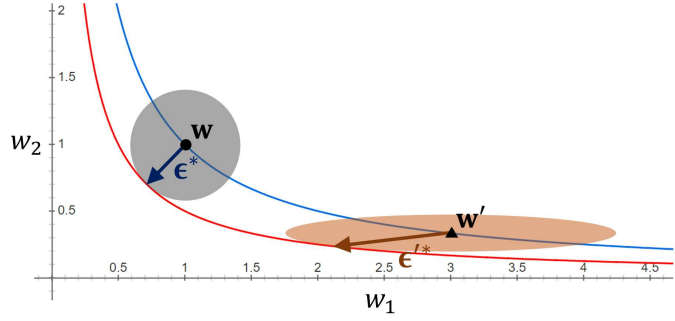
Definition 1 (Normalization operator). *Let $\{T_{\mathbf{w}}, \mathbf{w} \in \mathbb{R}^k\}$ be a family of invertible linear operators on \mathbb{R}^k . Given a weight \mathbf{w} , if $T_{A\mathbf{w}}^{-1}A = T_{\mathbf{w}}^{-1}$ for any invertible scaling operator A on \mathbb{R}^k which does not change the loss function, we say $T_{\mathbf{w}}^{-1}$ is a normalization operator of \mathbf{w} .*



(a) $\|\epsilon\|_2 \leq \rho$ and $\|\epsilon'\|_2 \leq \rho$ (Foret et al., 2020)



(b) $\|T_w^{-1}\epsilon\|_\infty \leq \rho$ and $\|T_{w'}^{-1}\epsilon'\|_\infty \leq \rho$ (Keskar et al., 2017)



(c) $\|T_w^{-1}\epsilon\|_2 \leq \rho$ and $\|T_{w'}^{-1}\epsilon'\|_2 \leq \rho$ (In this paper)

Figure 1: Loss contours and three types of maximization regions: (a) sphere, (b) cuboid and (c) ellipsoid. $\mathbf{w} = (1, 1)$ and $\mathbf{w}' = (3, 1/3)$ are parameter points before and after a -transformation with $a = 3$ and are expressed as dots and triangles, respectively. The blue contour line has the same loss at \mathbf{w} , and the red contour line has a loss equal to the maximum value of the loss in each type of region centered on \mathbf{w} . ϵ^* and ϵ'^* are the ϵ and ϵ' which maximize the loss perturbed from \mathbf{w} and \mathbf{w}' , respectively.

Using the normalization operator, we define adaptive sharpness as follows.

Definition 2 (Adaptive sharpness). *If $T_{\mathbf{w}}^{-1}$ is the normalization operator of \mathbf{w} in Definition 1, adaptive sharpness of \mathbf{w} is defined by*

$$\max_{\|T_{\mathbf{w}}^{-1}\epsilon\|_p \leq \rho} L_S(\mathbf{w} + \epsilon) - L_S(\mathbf{w}) \quad (4)$$

where $1 \leq p \leq \infty$.

Adaptive sharpness in Equation 4 has the following properties.

Theorem 1. *For any invertible scaling operator A which does not change the loss function, adaptive sharpnesses at \mathbf{w} and $A\mathbf{w}$ have the same value as*

$$\begin{aligned} & \max_{\|T_{\mathbf{w}}^{-1}\epsilon\|_p \leq \rho} L_S(\mathbf{w} + \epsilon) - L_S(\mathbf{w}) \\ &= \max_{\|T_{A\mathbf{w}}^{-1}\epsilon\|_p \leq \rho} L_S(A\mathbf{w} + \epsilon) - L_S(A\mathbf{w}) \end{aligned}$$

where $T_{\mathbf{w}}^{-1}$ and $T_{A\mathbf{w}}^{-1}$ are the normalization operators of \mathbf{w} and $A\mathbf{w}$ in Definition 1, respectively.

Proof. From the assumption, it suffices to show that the first terms of both sides are equal. By the definition of the normalization operator, we have $T_{A\mathbf{w}}^{-1}A = T_{\mathbf{w}}^{-1}$. Therefore,

$$\begin{aligned} \max_{\|T_{A\mathbf{w}}^{-1}\epsilon\|_p \leq \rho} L_S(A\mathbf{w} + \epsilon) &= \max_{\|T_{A\mathbf{w}}^{-1}\epsilon\|_p \leq \rho} L_S(\mathbf{w} + A^{-1}\epsilon) \\ &= \max_{\|T_{A\mathbf{w}}^{-1}A\epsilon'\|_p \leq \rho} L_S(\mathbf{w} + \epsilon') \\ &= \max_{\|T_{\mathbf{w}}^{-1}\epsilon'\|_p \leq \rho} L_S(\mathbf{w} + \epsilon') \end{aligned}$$

where $\epsilon' = A^{-1}\epsilon$. □

By Theorem 1, adaptive sharpness defined in Equation 4 is *scale-invariant* as with training loss and generalization loss. This property makes the correlation between adaptive sharpness and the generalization gap stronger than that of between sharpness in Equation 2 and generalization gap.

Figure 1(b) and 1(c) show how a re-scaled weight vector can have the same adaptive sharpness value as that of the original weight vector. It can be observed that the boundary line of each region centered on \mathbf{w}' is in contact with the red line. This implies that the maximum loss within each region centered on \mathbf{w}' is maintained when $\|T_{\mathbf{w}'}^{-1}\epsilon'\|_p \leq \rho$ is used for the maximization region. Thus, in this example, it can be seen that adaptive sharpness in 1(b) and 1(c) has scale-invariance property in contrast to sharpness of the spherical region shown in Figure 1(a).

The question that can be asked here is what kind of operators $T_{\mathbf{w}}$ can be considered as normalization operators which satisfy $T_{A\mathbf{w}}^{-1}A = T_{\mathbf{w}}^{-1}$ for any A which

does not change the loss function. As seen through the example in Section 3, one of the conditions for the scaling operator A that does not change the loss function is that it should be node-wise scaling, which corresponds to row-wise or column-wise scaling in fully-connected layers and channel-wise scaling in convolutional layers. The effect of such node-wise scaling can be canceled using the inverses of the following operators:

- element-wise

$$T_{\mathbf{w}} = \text{diag}(|w_1|, \dots, |w_k|)$$

where

$$\mathbf{w} = [w_1, w_2, \dots, w_k],$$

- filter-wise

$$T_{\mathbf{w}} = \text{diag}(\text{concat}(\|\mathbf{f}_1\|_2 \mathbf{1}_{n(\mathbf{f}_1)}, \dots, \|\mathbf{f}_m\|_2 \mathbf{1}_{n(\mathbf{f}_m)}, |w_1|, \dots, |w_q|)) \quad (5)$$

where

$$\mathbf{w} = \text{concat}(\mathbf{f}_1, \mathbf{f}_2, \dots, \mathbf{f}_m, w_1, w_2, \dots, w_q).$$

Here \mathbf{f}_i is the i -th flattened weight vector of a convolution filter and w_j is the j -th weight parameter which is not included in any filters. And m is the number of filters and q is the number of other weight parameters in the model. If there is no convolutional layer in a model (i.e., $m = 0$), then $q = k$ and both normalization operators are identical to each other. Note that we use $T_{\mathbf{w}} + \eta I_k$ rather than $T_{\mathbf{w}}$ for sufficiently small $\eta > 0$ for stability. η is a hyper-parameter controlling trade-off between adaptivity and stability.

To confirm that adaptive sharpness actually has a stronger correlation with generalization gap than sharpness, we compare scatter plots which demonstrate the change of adaptive sharpness and sharpness with respect to generalization gap. As can be seen in Figure 2, adaptive sharpness with generation gap shows better correlation than sharpness. The difference in correlation behaviors of adaptive sharpness and sharpness provides an evidence that scale invariance property of adaptive sharpness helps strengthen the correlation with generalization gap. The detailed information of these scatter plots is described in Appendix B.

Node-wise normalization can also be viewed as a normalization operator. Tsuzuku et al. (2020) suggest node-wise normalization method for obtaining normalized flatness. However, the method requires that the parameter should be at a critical point. Also, in the case of node-wise normalization using unit-invariant SVD (Uhlmann, 2018), there is a concern that the speed of the optimizer can degrade due to the significant additional cost for scale-direction decomposition of weight tensors. Therefore the node-wise normalization is not covered in this paper. In the case of layer-wise normalization using spectral norm or Frobenius norm of weight matrices (Neyshabur et al., 2017), the condition $T_{A\mathbf{w}}^{-1}A = T_{\mathbf{w}}^{-1}$ is not satisfied. Therefore, it cannot be used for adaptive sharpness so we do not cover it in this paper.

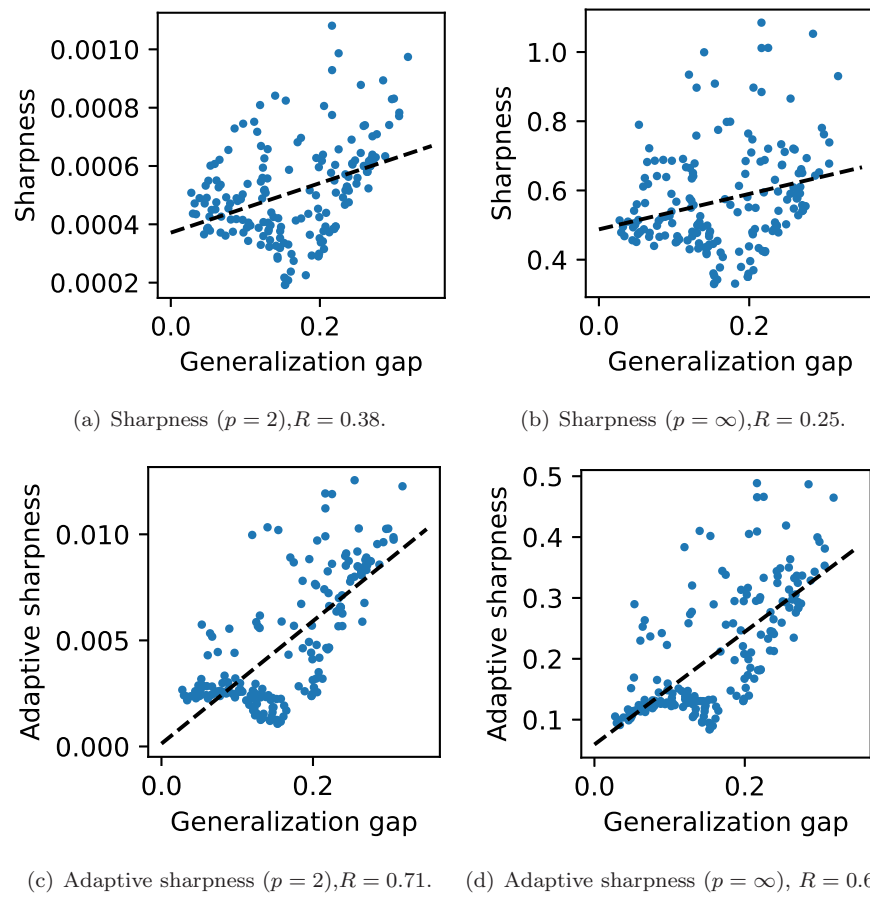


Figure 2: Scatter plots which show correlation of sharpness and adaptive sharpness with respect to generalization gap and their correlation coefficients R .

There are several previous works which are closely related to adaptive sharpness. Li et al. (2018), which suggest a methodology for visualizing loss landscape, is related to adaptive sharpness. In that study, filter-wise normalization which is equivalent to the definition in Equation 5 is used to remove scale dependency from loss landscape and make comparisons between loss functions meaningful. In spite of their empirical success, Li et al. (2018) do not provide a theoretical evidence for explaining how filter-wise scaling contributes the scale-invariance and correlation with generalization. In this paper, we clarify how the filter-wise normalization relates to generalization by proving the scale-invariant property of adaptive sharpness in Theorem 1.

Also, sharpness suggested in Keskar et al. (2017) can be regarded as a special case of adaptive sharpness which uses $p = \infty$ and the element-wise normalization operator. Jiang et al. (2019) confirm experimentally that cuboid region $\|T_{\mathbf{w}}^{-1}\epsilon\|_{\infty} \leq \rho$ which corresponds to adaptive sharpness with $p = \infty$ and the element-wise normalization operator shows a higher correlation with the generalization gap than square region $\|\epsilon\|_{\infty} \leq \rho$. This experimental result implies that Theorem 1 is also practically validated.

Therefore, it seems that sharpness with $p = \infty$ suggested by Keskar et al. (2017) also can be used directly for learning as it is, but a problem arises from the viewpoint of generalization performance. Foret et al. (2020) confirm experimentally that the generalization performance with sharpness defined in square region $\|\epsilon\|_{\infty} \leq \rho$ result is worse than when SAM is performed with sharpness defined in spherical region $\|\epsilon\|_2 \leq \rho$.

We conduct performance comparison tests for $p = 2$ and $p = \infty$, and experimentally revealed that $p = 2$ is more suitable for learning as in Foret et al. (2020). The experimental results for this are shown in Section 6.

5 Adaptive Sharpness-Aware Minimization

In the previous section, we introduce a scale-invariant measure called adaptive sharpness to overcome the limitation of sharpness. As in sharpness, we can obtain a generalization bound using adaptive sharpness, which is presented in the following theorem.

Theorem 2. *Let $T_{\mathbf{w}}^{-1}$ be the normalization operator on \mathbb{R}^k . If $L_D(\mathbf{w}) \leq E_{\epsilon_i \sim \mathcal{N}(0, \sigma^2)}[L_D(\mathbf{w} + \epsilon)]$ for some $\sigma > 0$, then with probability $1 - \delta$,*

$$L_D(\mathbf{w}) \leq \max_{\|T_{\mathbf{w}}^{-1}\epsilon\|_2 \leq \rho} L_S(\mathbf{w} + \epsilon) + h\left(\frac{\|\mathbf{w}\|_2^2}{\eta^2 \rho^2}\right), \quad (6)$$

where $h : \mathbb{R}^+ \rightarrow \mathbb{R}^+$ is a strictly increasing function, $n = |S|$ and $\rho = \sqrt{k}\sigma(1 + \sqrt{\log n/k})/\eta$.

Note that Theorem 2 still holds for $p > 2$ due to the monotonicity of p -norm, i.e., if $0 < r < p$, $\|\mathbf{x}\|_p \leq \|\mathbf{x}\|_r$ for any $\mathbf{x} \in \mathbb{R}^n$. If $T_{\mathbf{w}}$ is an identity operator,

Equation 6 is reduced equivalently to Equation 1. The proof of Equation 6 is described in detail in Appendix A.1.

The right hand side of Equation 6, i.e., generalization bound, can be expressed using adaptive sharpness as

$$\left(\max_{\|T_{\mathbf{w}}^{-1}\boldsymbol{\epsilon}\|_p \leq \rho} L_S(\mathbf{w} + \boldsymbol{\epsilon}) - L_S(\mathbf{w}) \right) + L_S(\mathbf{w}) + h\left(\frac{\|\mathbf{w}\|_2^2}{\eta^2 \rho^2}\right).$$

Since $h\left(\|\mathbf{w}\|_2^2/\eta^2 \rho^2\right)$ is a monotonically increasing function with respect to $\|\mathbf{w}\|_2^2$, it can be substituted with ℓ^2 weight decaying regularizer. Therefore, we can define adaptive sharpness-aware minimization problem as

$$\min_{\mathbf{w}} \max_{\|T_{\mathbf{w}}^{-1}\boldsymbol{\epsilon}\|_p \leq \rho} L_S(\mathbf{w} + \boldsymbol{\epsilon}) + \frac{\lambda}{2} \|\mathbf{w}\|_2^2. \quad (7)$$

To solve the minimax problem in Equation 7, it is necessary to first find optimal $\boldsymbol{\epsilon}$. Analogous to SAM, we can approximate the optimal $\boldsymbol{\epsilon}$ to maximize $L_S(\mathbf{w} + \boldsymbol{\epsilon})$ using a first-order approximation as

$$\begin{aligned} \tilde{\boldsymbol{\epsilon}}_t &= \arg \max_{\|\tilde{\boldsymbol{\epsilon}}\|_p \leq \rho} L_S(\mathbf{w}_t + T_{\mathbf{w}_t} \tilde{\boldsymbol{\epsilon}}) \\ &\approx \arg \max_{\|\tilde{\boldsymbol{\epsilon}}\|_p \leq \rho} \tilde{\boldsymbol{\epsilon}}^\top T_{\mathbf{w}_t} \nabla L_S(\mathbf{w}_t) \\ &= \rho \operatorname{sign}(\nabla L_S(\mathbf{w}_t)) \frac{|T_{\mathbf{w}_t} \nabla L_S(\mathbf{w}_t)|^{q-1}}{\|T_{\mathbf{w}_t} \nabla L_S(\mathbf{w}_t)\|_q^{q-1}}, \end{aligned}$$

where $\tilde{\boldsymbol{\epsilon}} = T_{\mathbf{w}}^{-1}\boldsymbol{\epsilon}$. Then, the two-step procedure for adaptive sharpness-aware minimization (ASAM) is expressed as

$$\begin{cases} \boldsymbol{\epsilon}_t = \rho T_{\mathbf{w}_t} \operatorname{sign}(\nabla L_S(\mathbf{w}_t)) \frac{|T_{\mathbf{w}_t} \nabla L_S(\mathbf{w}_t)|^{q-1}}{\|T_{\mathbf{w}_t} \nabla L_S(\mathbf{w}_t)\|_q^{q-1}} \\ \mathbf{w}_{t+1} = \mathbf{w}_t - \alpha_t (\nabla L_S(\mathbf{w}_t + \boldsymbol{\epsilon}_t) + \lambda \mathbf{w}_t) \end{cases}$$

for $t = 0, 1, 2, \dots$. Especially, if $p = 2$,

$$\boldsymbol{\epsilon}_t = \rho \frac{T_{\mathbf{w}_t}^2 \nabla L_S(\mathbf{w}_t)}{\|T_{\mathbf{w}_t} \nabla L_S(\mathbf{w}_t)\|_2},$$

and if $p = \infty$,

$$\boldsymbol{\epsilon}_t = \rho T_{\mathbf{w}_t} \operatorname{sign}(\nabla L_S(\mathbf{w}_t)).$$

In this study, experiments were conducted on ASAM in cases of $p = \infty$ and $p = 2$. The ASAM algorithm with $p = 2$ is described in detail on Algorithm 1.

6 Experimental Results

In this section, we evaluate the performance of ASAM. We first show how SAM and ASAM operate differently in a toy example. We then compare the generalization performance of ASAM with SGD and SAM for various model architectures and CIFAR10 and CIFAR100 datasets (Krizhevsky et al., 2009). Finally, we show how robust to label noise SAM and ASAM algorithms are.

Algorithm 1 ASAM algorithm ($p = 2$)

Input: Loss function l , training dataset $S := \cup_{i=1}^n \{(\mathbf{x}_i, \mathbf{y}_i)\}$, batch size b , radius of maximization region ρ , weight decaying factor λ , scheduled learning rate α , initial weight \mathbf{w}_0 .

Output: Trained weight \mathbf{w}

Initialize weight $\mathbf{w} := \mathbf{w}_0$

while not converged **do**

- Sample a mini-batch B of size b from S
- $\epsilon := \rho \frac{T_{\mathbf{w}}^2 \nabla L_B(\mathbf{w})}{\|T_{\mathbf{w}} \nabla L_B(\mathbf{w})\|_2}$
- $\mathbf{w} := \mathbf{w} - \alpha (\nabla L_B(\mathbf{w}) + \epsilon) + \lambda \mathbf{w}$

end while

return \mathbf{w}

6.1 Toy Example

As mentioned in Section 3, sharpness varies by parameter re-scaling even if its loss function remains the same, while adaptive sharpness does not. To elaborate this, we consider a simple loss function $L(\mathbf{w}) = |w_1 \text{ReLU}(w_2) - 0.04|$ where $\mathbf{w} = (w_1, w_2) \in \mathbb{R}^2$. Figure 3 presents the trajectories of SAM and ASAM with two different initial weights $\mathbf{w}_0 = (0.2, 0.05)$ and $\mathbf{w}_0 = (0.3, 0.033)$. The red line represents the set of minimizers of the loss function L , i.e., $\{(w_1, w_2); w_1 w_2 = 0.04, w_2 > 0\}$. As seen in Figure 1(a), sharpness is maximized when $w_1 = w_2$ within the same loss contour line, and therefore SAM tries to converge to $(0.2, 0.2)$. Here, we use $\rho = 0.05$ as in Foret et al. (2020). On the other hand, adaptive sharpness remains the same along the same contour line which implies that ASAM converges to the point in the red line near the initial point as can be seen in Figure 3.

Since SAM minimizes sharpness in a spherical region with a fixed radius, it may cause undesirable results depending on the loss surface and the current weight. If $\mathbf{w}_0 = (0.3, 0.033)$, while SAM fails to converge to the valley even with $\rho = 0.05$, ASAM still converges.

6.2 CIFAR10 and CIFAR100

To confirm the effectiveness of ASAM, we conduct comparison experiments with SAM using CIFAR10 and CIFAR100 datasets and we use the same data split as the original paper. The hyper-parameters used in this test is described in Table 2. Before the comparison tests with SAM, there are two factors to be chosen in ASAM algorithm:

- Normalization schemes: Filter-wise vs. Element-wise
- p -norm: $p = \infty$ vs. $p = 2$

First, we perform the comparison test for filter-wise and element-wise normalization using WideResNet-16-8 model (Zagoruyko & Komodakis, 2016) and

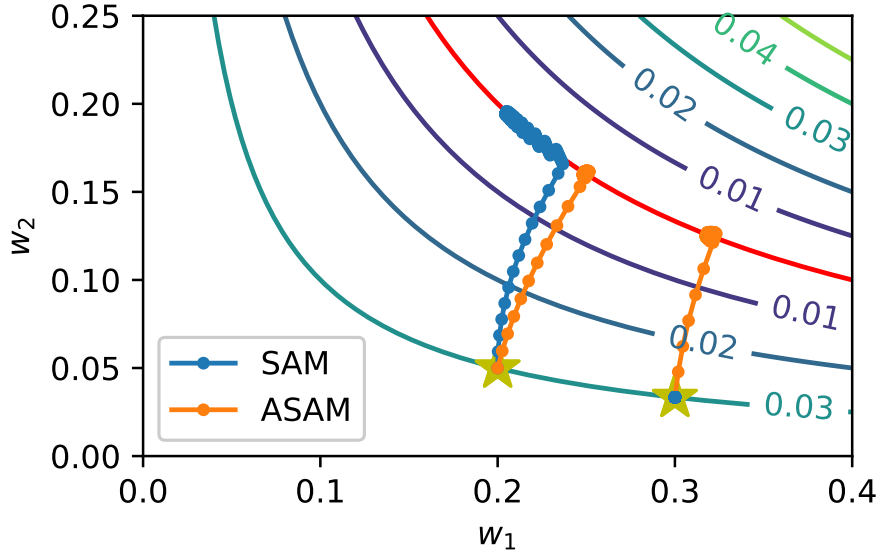


Figure 3: Trajectories of SAM and ASAM.

illustrate the results in Figure 4. As can be seen, both test accuracies are comparable across ρ . Since element-wise normalization provides a slightly better accuracy at $\rho = 1.0$, we decide to use the element-wise normalization in the remaining tests.

Similarly, Figure 4 shows how much test accuracy varies with the maximization region for adaptive sharpness. In Foret et al. (2020), they empirically confirm $p = 2$ shows better test accuracies than $p = \infty$ does. Consistently with the results of their tests, we confirm that $p = 2$ also shows better accuracies than $p = \infty$. Thus, we determine to use $p = 2$ as the maximization region for adaptive sharpness.

As ASAM has a hyper-parameter ρ to be tuned, we first conduct a grid search over $\{0.00005, 0.0001, 0.0002, \dots, 0.5, 1.0, 2.0\}$ for finding appropriate values of ρ . We use $\rho = 0.5$ for CIFAR10 and $\rho = 1.0$ for CIFAR100 for the remaining tests, because it gives moderately good performance across various models. We set ρ for SAM as 0.05 for CIFAR10 and 0.1 for CIFAR100 as in Foret et al. (2020). η for ASAM is set to 0.01. Mini batch size is 128, and m -sharpness suggested by Foret et al. (2020) is not employed. The number of epochs is 200 for SAM and ASAM and 400 for SGD. Momentum and weight decay factor is set to 0.9 and 0.0005. The rest of the hyperparameters are the same with Appendix B.

Using the hyper-parameters, we compare the best test accuracies obtained by SGD (Nesterov, 1983), SAM and ASAM for various rectifier neural network models: VGG (Simonyan & Zisserman, 2014), ResNet (He et al., 2016),

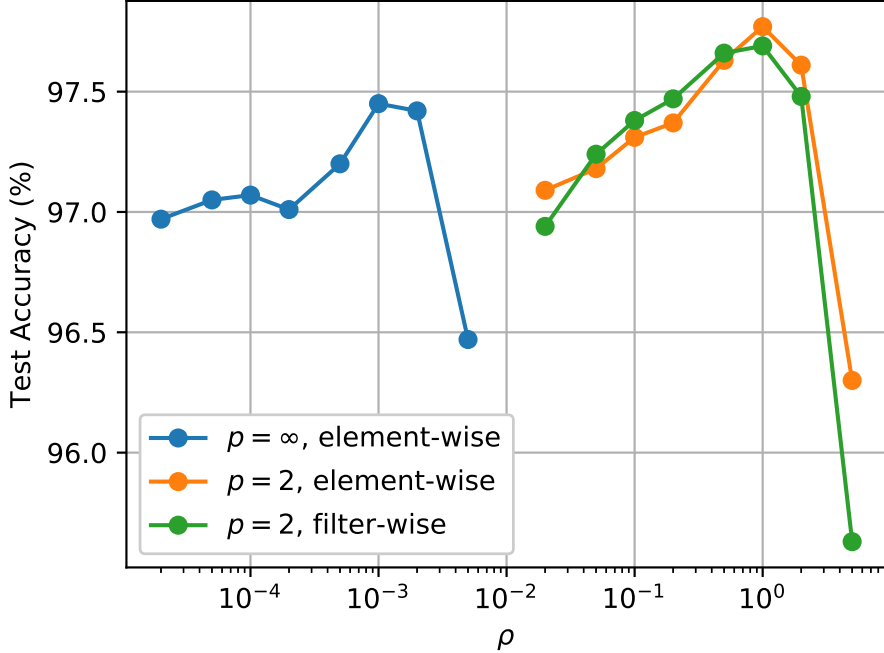


Figure 4: Test accuracy curves obtained from ASAM algorithm using a range of ρ with different p and normalization schemes: element-wise normalization with $p = \infty$, element-wise normalization with $p = 2$ and filter-wise normalization with $p = 2$.

DenseNet (Huang et al., 2017), WideResNet (Zagoruyko & Komodakis, 2016), and ResNeXt (Xie et al., 2017). In both CIFAR10 and CIFAR100 cases, ASAM generally surpasses SGD and SAM, as can be seen in Table 1 and Table 2. Every entry in the tables represents mean and standard deviation of 5 independent runs. These results imply that ASAM can enhance generalization performance of rectifier neural network architectures in image classification task.

6.3 Robustness to Label Noise

SAM is robust to label noise in the training data, as it has shown its robustness comparable to MentorMix (Jiang et al., 2020), which is a state of the art method. We expect that ASAM would share the robustness to label noise. To confirm this, we compare the test accuracies of SGD, SAM and ASAM for ResNet-32 model and CIFAR10 dataset whose labels in the training data are corrupted by symmetric label noise (Van Rooyen et al., 2015) with noise levels of 20%, 40%, 60% and 80%, and the test data is not touched. Hyper-parameter settings are

Table 1: Maximum test accuracies for SGD, SAM and ASAM on CIFAR-10 dataset.

Model	SGD	SAM	ASAM
WRN-28-10	96.34 \pm 0.12	96.98 \pm 0.04	97.28 \pm 0.07
WRN-28-2	95.13 \pm 0.16	95.74 \pm 0.08	95.94 \pm 0.05
ResNeXt29-32x4d	95.84 \pm 0.24	96.34 \pm 0.30	96.80 \pm 0.06
DenseNet121	91.00 \pm 0.13	92.00 \pm 0.17	93.33 \pm 0.04
ResNet56	94.58 \pm 0.20	95.18 \pm 0.15	95.42 \pm 0.16
ResNet20	93.18 \pm 0.21	93.56 \pm 0.15	93.82 \pm 0.17
VGG19-BN*	93.87 \pm 0.09	94.60	95.07 \pm 0.05

* Some runs completely failed, thus giving 10% of accuracy
(success rate: SGD: 3/5, SAM 1/5, ASAM 3/5)

Table 2: Maximum test accuracies for SGD, SAM and ASAM on CIFAR-100 dataset.

Model	SGD	SAM	ASAM
WRN-28-10	81.56 \pm 0.13	83.42 \pm 0.04	83.68 \pm 0.12
WRN-28-2	75.28 \pm 0.17	77.25 \pm 0.35	77.54 \pm 0.14
ResNeXt29-32x4d	79.76 \pm 0.23	81.48 \pm 0.17	82.30 \pm 0.11
DenseNet121	68.70 \pm 0.31	69.84 \pm 0.12	70.60 \pm 0.20
ResNet56	73.12 \pm 0.19	75.16 \pm 0.05	75.86 \pm 0.22
ResNet20	69.76 \pm 0.44	71.06 \pm 0.31	71.40 \pm 0.30
VGG19-BN*	71.80 \pm 1.35	73.52 \pm 1.74	75.80 \pm 0.27

* Some runs completely failed, thus giving 10% of accuracy
(success rate: SGD: 5/5, SAM 4/5, ASAM 4/5)

the same as that of previous experiments. The results of the experiments are obtained from three independent runs. Table 3 shows test accuracies for SGD, SAM and ASAM with respect to label noise levels. Compared to SAM, ASAM generally enhances the test accuracy across various noise level, while retaining the robustness to label noise.

Table 3: Maximum test accuracies of ResNet-32 models trained on CIFAR-10 with label noise.

Noise rate	SGD	SAM	ASAM
0%	94.50 ± 0.11	94.80 ± 0.12	94.88 ± 0.12
20%	91.32 ± 0.23	92.94 ± 0.12	93.21 ± 0.10
40%	87.68 ± 0.05	90.62 ± 0.18	90.89 ± 0.13
60%	82.50 ± 0.30	86.58 ± 0.30	87.41 ± 0.16
80%	68.35 ± 0.85	69.92 ± 0.98	67.69 ± 1.34

7 Conclusions

In this paper, we have introduced adaptive sharpness whose scale invariance property improves training path in weight space by adjusting their maximization region with respect to weight scale. Also, we have confirmed empirically that this property, which ASAM also has, contributes the improvement of generalization performance. The surpassing performance of ASAM is notable in that the comparison tests are conducted with SAM, which is known as a currently state-of-the-art learning algorithm in many image-classification benchmarks. In addition to the contribution as learning algorithm, adaptive sharpness can serve as a generalization measure due to stronger correlation with generalization gap benefiting from their scale-invariant property. So adaptive sharpness has a potential to be a metric for assessment of neural networks. We have also suggested the condition of normalization operator for adaptive sharpness but we do not cover all the normalization schemes which satisfy the condition. So this area is expected to be more investigated for better generalization performance in the future work.

References

Chatterji, N., Neyshabur, B., and Sedghi, H. The intriguing role of module criticality in the generalization of deep networks. In *International Conference on Learning Representations*, 2019.

Chaudhari, P., Choromanska, A., Soatto, S., LeCun, Y., Baldassi, C., Borgs, C., Chayes, J., Sagun, L., and Zecchina, R. Entropy-sgd: Biasing gradient descent into wide valleys. *Journal of Statistical Mechanics: Theory and Experiment*, 2019(12):124018, 2019.

DeVries, T. and Taylor, G. W. Improved regularization of convolutional neural networks with cutout. *arXiv preprint arXiv:1708.04552*, 2017.

Dinh, L., Pascanu, R., Bengio, S., and Bengio, Y. Sharp minima can generalize for deep nets. In *International Conference on Machine Learning*, pp. 1019–1028. PMLR, 2017.

Foret, P., Kleiner, A., Mobahi, H., and Neyshabur, B. Sharpness-aware minimization for efficiently improving generalization. *arXiv preprint arXiv:2010.01412*, 2020.

He, K., Zhang, X., Ren, S., and Sun, J. Deep residual learning for image recognition. In *Proceedings of the IEEE conference on computer vision and pattern recognition*, pp. 770–778, 2016.

Hochreiter, S. and Schmidhuber, J. Flat minima. *Neural computation*, 9(1):1–42, 1997.

Hochreiter, S., Schmidhuber, J., et al. Simplifying neural nets by discovering flat minima. *Advances in neural information processing systems*, pp. 529–536, 1995.

Huang, G., Liu, Z., Van Der Maaten, L., and Weinberger, K. Q. Densely connected convolutional networks. In *Proceedings of the IEEE conference on computer vision and pattern recognition*, pp. 4700–4708, 2017.

Jiang, L., Huang, D., Liu, M., and Yang, W. Beyond synthetic noise: Deep learning on controlled noisy labels. In *International Conference on Machine Learning*, pp. 4804–4815. PMLR, 2020.

Jiang, Y., Neyshabur, B., Mobahi, H., Krishnan, D., and Bengio, S. Fantastic generalization measures and where to find them. In *International Conference on Learning Representations*, 2019.

Karakida, R., Akaho, S., and Amari, S.-i. The normalization method for alleviating pathological sharpness in wide neural networks. *arXiv preprint arXiv:1906.02926*, 2019.

Keskar, N. S., Nocedal, J., Tang, P. T. P., Mudigere, D., and Smelyanskiy, M. On large-batch training for deep learning: Generalization gap and sharp minima. In *5th International Conference on Learning Representations, ICLR 2017*, 2017.

Krizhevsky, A., Nair, V., and Hinton, G. Cifar-10 and cifar-100 datasets. *URL: <https://www.cs.toronto.edu/kriz/cifar.html>*, 6(1):1, 2009.

Laurent, B. and Massart, P. Adaptive estimation of a quadratic functional by model selection. *Annals of Statistics*, pp. 1302–1338, 2000.

Li, H., Xu, Z., Taylor, G., Studer, C., and Goldstein, T. Visualizing the loss landscape of neural nets. In *NIPS'18: Proceedings of the 32nd International Conference on Neural Information Processing Systems*, pp. 6391–6401. Curran Associates Inc., 2018.

Liang, T., Poggio, T., Rakhlin, A., and Stokes, J. Fisher-rao metric, geometry, and complexity of neural networks. In *The 22nd International Conference on Artificial Intelligence and Statistics*, pp. 888–896. PMLR, 2019.

Loshchilov, I. and Hutter, F. Sgdr: Stochastic gradient descent with warm restarts. *arXiv preprint arXiv:1608.03983*, 2016.

McAllester, D. A. Pac-bayesian model averaging. In *Proceedings of the twelfth annual conference on Computational learning theory*, pp. 164–170, 1999.

Mobahi, H. Training recurrent neural networks by diffusion. *arXiv preprint arXiv:1601.04114*, 2016.

Müller, R., Kornblith, S., and Hinton, G. When does label smoothing help? *arXiv preprint arXiv:1906.02629*, 2019.

Nesterov, Y. E. A method for solving the convex programming problem with convergence rate $o(1/k^2)$. In *Dokl. akad. nauk Sssr*, volume 269, pp. 543–547, 1983.

Neyshabur, B., Bhojanapalli, S., McAllester, D., and Srebro, N. Exploring generalization in deep learning. *arXiv preprint arXiv:1706.08947*, 2017.

Simonyan, K. and Zisserman, A. Very deep convolutional networks for large-scale image recognition. *arXiv preprint arXiv:1409.1556*, 2014.

Sun, X., Zhang, Z., Ren, X., Luo, R., and Li, L. Exploring the vulnerability of deep neural networks: A study of parameter corruption. *arXiv preprint arXiv:2006.05620*, 2020.

Tsuzuku, Y., Sato, I., and Sugiyama, M. Normalized flat minima: Exploring scale invariant definition of flat minima for neural networks using pac-bayesian analysis. In *International Conference on Machine Learning*, pp. 9636–9647. PMLR, 2020.

Uhlmann, J. A generalized matrix inverse that is consistent with respect to diagonal transformations. *SIAM Journal on Matrix Analysis and Applications*, 39(2):781–800, 2018.

Van Rooyen, B., Menon, A. K., and Williamson, R. C. Learning with symmetric label noise: The importance of being unhinged. *arXiv preprint arXiv:1505.07634*, 2015.

Xie, S., Girshick, R., Dollár, P., Tu, Z., and He, K. Aggregated residual transformations for deep neural networks. In *Proceedings of the IEEE conference on computer vision and pattern recognition*, pp. 1492–1500, 2017.

Yi, M., Meng, Q., Chen, W., Ma, Z.-m., and Liu, T.-Y. Positively scale-invariant flatness of relu neural networks. *arXiv preprint arXiv:1903.02237*, 2019.

Yue, X., Nouiehed, M., and Kontar, R. A. Salr: Sharpness-aware learning rates for improved generalization. *arXiv preprint arXiv:2011.05348*, 2020.

Zagoruyko, S. and Komodakis, N. Wide residual networks. *arXiv preprint arXiv:1605.07146*, 2016.

A Proofs

A.1 Proof of Theorem 2

We first introduce the following concentration inequality.

Lemma 1. *Let $\{\epsilon_i, i = 1, \dots, k\}$ be independent normal variables with mean 0 and variance σ_i^2 . Then,*

$$P \left(\sum_{i=1}^k \epsilon_i^2 \geq k\sigma_{\max}^2 \left(1 + \sqrt{\frac{\log n}{k}} \right)^2 \right) \leq \frac{1}{\sqrt{n}}$$

where $\sigma_{\max} = \max\{\sigma_i\}$.

Proof. From Lemma 1 in Laurent & Massart (2000), for any $x > 0$,

$$P \left(\sum_{i=1}^k \epsilon_i^2 \geq \sum_{i=1}^k \sigma_i^2 + 2\sqrt{\sum_{i=1}^k \sigma_i^4 x} + 2\sigma_{\max}^2 x \right) \leq \exp(-x).$$

Since

$$\begin{aligned} \sum_{i=1}^k \sigma_i^2 + 2\sqrt{\sum_{i=1}^k \sigma_i^4 x} + 2\sigma_{\max}^2 x &\leq \sigma_{\max}^2 (k + 2\sqrt{kx} + 2x) \\ &\leq \sigma_{\max}^2 (\sqrt{k} + \sqrt{2x})^2, \end{aligned}$$

plugging $x = \frac{1}{2} \log n$ proves the lemma. \square

Theorem 3. *Let $T_{\mathbf{w}}^{-1}$ be the filter-wise normalization operator of \mathbf{w} on \mathbb{R}^k . If $L_D(\mathbf{w}) \leq E_{\epsilon_i \sim \mathcal{N}(0, \sigma^2)}[L_D(\mathbf{w} + \epsilon)]$ for some $\sigma > 0$, then with probability $1 - \delta$,*

$$\begin{aligned} L_D(\mathbf{w}) &\leq \max_{\|T_{\mathbf{w}}^{-1}\epsilon\|_2 \leq \rho} L_S(\mathbf{w} + \epsilon) \\ &\quad + \sqrt{\frac{1}{n-1} \left(k \log \left(1 + \frac{\|\mathbf{w}\|_2^2}{\eta^2 \rho^2} \left(1 + \sqrt{\frac{\log n}{k}} \right)^2 \right) + 4 \log \frac{n}{\delta} + O(1) \right)} \end{aligned}$$

where $n = |S|$ and $\rho = \sqrt{k}\sigma(1 + \sqrt{\log n/k})/\eta$.

Proof. The idea of the proof is given in Foret et al. (2020). From the assumption, adding Gaussian perturbation on the weight space does not improve the test error. Moreover, from Theorem 3.2 in Chatterji et al. (2019), the following generalization bound holds under the perturbation:

$$\begin{aligned} E_{\epsilon_i \sim \mathcal{N}(0, \sigma^2)}[L_D(\mathbf{w} + \epsilon)] &\leq E_{\epsilon_i \sim \mathcal{N}(0, \sigma^2)}[L_S(\mathbf{w} + \epsilon)] \\ &\quad + \sqrt{\frac{1}{n-1} \left(\frac{1}{4} k \log \left(1 + \frac{\|\mathbf{w}\|_2^2}{k\sigma^2} \right) + \log \frac{n}{\delta} + C(n, \sigma, k) \right)}. \end{aligned}$$

Therefore, the left hand side of the statement can be bounded as

$$\begin{aligned}
L_D(\mathbf{w}) &\leq E_{\epsilon_i \sim \mathcal{N}(0, \sigma^2)}[L_S(\mathbf{w} + \epsilon)] \\
&+ \sqrt{\frac{1}{n-1} \left(\frac{1}{4} k \log \left(1 + \frac{\|\mathbf{w}\|_2^2}{k\sigma^2} \right) + \log \frac{n}{\delta} + C \right)} \\
&\leq \left(1 - \frac{1}{\sqrt{n}} \right) \max_{\|T_{\mathbf{w}}^{-1}\epsilon\|_2 \leq \rho} L_S(\mathbf{w} + \epsilon) + \frac{1}{\sqrt{n}} \\
&+ \sqrt{\frac{1}{n-1} \left(\frac{1}{4} k \log \left(1 + \frac{\|\mathbf{w}\|_2^2}{k\sigma^2} \right) + \log \frac{n}{\delta} + C \right)} \\
&\leq \max_{\|T_{\mathbf{w}}^{-1}\epsilon\|_2 \leq \rho} L_S(\mathbf{w} + \epsilon) + \sqrt{\frac{1}{n-1} \left(k \log \left(1 + \frac{\|\mathbf{w}\|_2^2}{k\sigma^2} \right) + 4 \log \frac{n}{\delta} + 4C \right)}
\end{aligned}$$

where the second inequality follows from Lemma 1 and $\|T_{\mathbf{w}}^{-1}\|_2 \leq \frac{1}{\eta}$. \square

B Correlation between Adaptive Sharpness and Generalization Gap

For this comparison test, we use WideResNet-16-8 model trained on CIFAR10 dataset. To obtain model parameters with various generalization gaps for well-distributed scatter plots, we train model parameters with various weight decay factors, which are expected to provide different generalization performance. The 9 weight decay factors used for training models are $\{1e-6, 2e-6, 5e-6, 1e-5, 2e-5, 5e-5, 1e-4, 2e-4, 5e-4\}$. We pick model parameters at every 10th epoch during each training procedure so the total number of trained models used for generating scatter plots is 180. Using these model parameters, we calculate sharpness and adaptive sharpness with respect to generalization gap.

To generate the trained models, we set mini-batch size to 256 and the number of epochs is 200. Cosine learning rate decay (Loshchilov & Hutter, 2016) is adopted with 0.1 initial learning rate. Also, random resize, padding by four pixels, normalization, random horizontal flip and cutout (DeVries & Taylor, 2017) are applied for data augmentation and label smoothing (Müller et al., 2019) is adopted with its factor of 0.1.

To calculate adaptive sharpness, we fix normalization scheme to element-wise normalization. We plot adaptive sharpness and sharpness with both $p = 2$ and $p = \infty$. We conduct a grid search over $\{1e-5, 2e-5, 5e-5, 1e-4, 2e-4, 5e-4, 1e-3, 2e-3, 5e-3, 1e-2, 2e-2, 5e-2\}$ to obtain each ρ for sharpness and adaptive sharpness which maximizes correlation with generalization gap. As results of the grid search, we select $1e-4$ and $5e-5$ as ρ s for sharpness of $p = 2$ and $p = \infty$, respectively, and select $5e-3$ and $5e-4$ as ρ s for adaptive sharpness of $p = 2$ and $p = \infty$, respectively. To calculate maximizers of each loss function, we follow m -sharpness strategy suggested by Foret et al. (2020) and m is set to 8.